nature structural & molecular biology

Structural perspective on the activation of RNase P RNA by protein

Amy H Buck[1], Alexei V Kazantsev[2], Andrew B Dalby[2] & Norman R Pace[2]

Ribonucleoprotein particles are central to numerous cellular pathways, but their study *in vitro* is often complicated by heterogeneity and aggregation. We describe a new technique to characterize these complexes trapped as homogeneous species in a nondenaturing gel. Using this technique, in conjunction with phosphorothioate footprinting analysis, we identify the protein-binding site and RNA folding states of ribonuclease P (RNase P), an RNA-based enzyme that, *in vivo*, requires a protein cofactor to catalyze the 5′ maturation of precursor transfer RNA (pre-tRNA). Our results show that the protein binds to a patch of conserved RNA structure adjacent to the active site and influences the conformation of the RNA near the tRNA-binding site. The data are consistent with a role of the protein in substrate recognition and support a new model of the holoenzyme that is based on a recently solved crystal structure of RNase P RNA.

The partnership of RNA and protein components is essential for the function of ribonucleoproteins, but the molecular interactions that define this partnership are often unclear. In bacterial RNase P, only one RNA and one protein compose the active holoenzyme, which catalyzes a phosphodiester hydrolysis that removes the 5′ leader sequence of pre-tRNA. Under conditions of elevated ionic strength *in vitro*, the RNA (~130 kDa) can perform catalysis in the absence of the protein (~14 kDa), but the protein is required *in vivo* and under physiological conditions *in vitro*[1,2]. The protein has been shown to influence substrate recognition by RNase P[3]; we earlier proposed that it activates the RNase P RNA structure required for efficient substrate binding[4]. In the current study we examine the structural basis for activation of RNase P RNA by RNase P protein.

The crystal structure of the *Bacillus stearothermophilus* RNase P RNA was recently solved at a resolution of 3.3 Å and provides the highest resolution model for the RNase P ribozyme[5]. High-resolution structures of the RNase P protein are available, but there is no high-resolution structure of the RNase P holoenzyme, the active species *in vivo*. Previous footprinting studies with *Bacillus subtilis* RNase P RNA (~80% identity with *B. stearothermophilus* RNase P RNA) indicate that several domains of the RNA are influenced by the protein[6,7], but analyses with the catalytic domain suggest that this domain of the RNA contains the protein-binding site[8,9]. The protein recognition elements are expected to be conserved in RNAs from diverse bacteria (the *B. subtilis* protein can complement the *Escherichia coli* RNA and vice versa)[1,4,10]; however, there is little overlap in the data with respect to the protein-binding site in *B. subtilis* and *E. coli* RNase P RNAs[6,9,11–14], with noted exceptions[7,15,16].

To derive a robust model for the interaction between RNA and protein in RNase P, we conducted a comparative footprinting analysis. We assume that many of the previous footprinting studies with RNase P could have been complicated by nonspecific binding of excess RNase P protein[12], large conformational changes in RNase P RNA[13] and/or dimerization of the holoenzyme[4,17]. To eliminate these caveats, we developed an in-gel phosphorothioate-iodine footprinting assay to probe the RNA and holoenzyme structures in their homogeneous, monomeric forms. Using this technique, we examined *E. coli* and *B. stearothermophilus* RNase P RNAs in the presence of *E. coli*, *B. subtilis* and *Thermotoga maritima* RNase P proteins. The rationale for comparing the two RNAs derives from substantial differences between the secondary structures of the *E. coli* and *B. stearothermophilus* RNAs, which are grouped into A (ancestral) and B (bacillus) types, respectively[18,19]. However, the structures of the RNase P proteins are highly conserved[20], so comparison of the protein footprints provides an important test for the generality or idiosyncrasy of our results.

Here we identify the protein-binding sites in A- and B-type RNAs, and we map the data onto the recently determined crystal structure of the *B. stearothermophilus* RNA. The results show that phylogenetically diverse proteins all bind to the same local patch of conserved RNA structure, adjacent to the proposed active site. Using the in-gel phosphorothioate-iodine assay, we also identify the specific tertiary elements in the RNA that stabilize the global structure and examine the spatial relationship between these elements and the protein-binding site.

RESULTS

Specificity of the RNA-protein interaction

The binding affinities of *E. coli*, *B. subtilis* and *T. maritima* RNase P proteins for both their cognate and noncognate RNAs were examined

[1]Department of Chemistry and Biochemistry and [2]Department of Molecular Cellular and Developmental Biology, University of Colorado, Boulder, Colorado 80309, USA. Correspondence should be addressed to N.R.P. (norman.pace@colorado.edu).

Received 5 July; accepted 13 September; published online 16 October 2005; doi:10.1038/nsmb1004

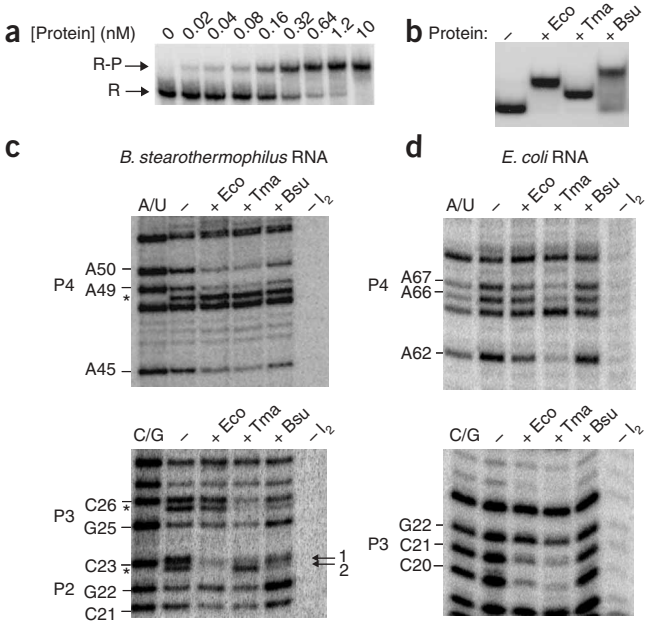

Figure 1 Nondenaturing gel shift and phosphorothioate-iodine protection of RNase P RNA by RNase P protein. (**a**) Nondenaturing gel of *B. stearothermophilus* catalytic-domain RNA (0.05 nM) titrated with 0–10 nM *E. coli* protein. Free RNA is labeled R, and RNA bound by protein is labeled R-P. (**b**) Nondenaturing gel with *B. stearothermophilus* catalytic-domain RNA (with random phosphorothioate incorporation) and equimolar *E. coli* (Eco), *T. maritima* (Tma) or *B. subtilis* (Bsu) protein. (**c**) Iodine cleavage pattern of RNA from each gel band shown in **b**. The first lane is denatured RNA (A/U and C/G denote which phosphorothioates are incorporated in the RNA in each panel); the next lanes are RNA in the absence (–) or presence (+) of each of the proteins, and the last lane ($-I_2$) is RNA that was not incubated with iodine. The residues that show an altered cleavage pattern in the presence of protein are indicated with the helix (for example, P4) in which they reside. The asterisks indicate residues that yield two reaction products. For residue C23, the two products of the reaction are labeled 1 and 2. (**d**) Cleavage pattern of *E. coli* catalytic-domain RNA with each of the proteins, as in **c**.

using a nondenaturing gel shift assay. The proteins bind to A-type (*E. coli*) and B-type (*B. subtilis* and *B. stearothermophilus*) RNase P RNAs with comparable affinities ($K_d \approx 0.2$–0.6 nM) and show no appreciable preference for cognate versus noncognate RNA (data not shown). (The *T. maritima* RNase P RNA was excluded from the analysis because of its conformational heterogeneity *in vitro*.) These K_d values agree with the previously reported K_d for the *E. coli* protein binding to *E. coli* RNA ($\sim$0.4 nM)[12] and suggest that all the proteins recognize structural elements that are shared among the different RNAs. The 263-nucleotide (nt) catalytic domain of *B. stearothermophilus* RNA is necessary and sufficient for protein binding ($K_d \approx$ 0.3 nM, **Fig. 1a**), consistent with a recent report[8]. All of the RNase P proteins examined bind the RNAs in a 1:1 ratio, but they result in slightly different gel mobilities of the holoenzymes (**Fig. 1b**). The differences in gel mobilities could result from variations in the exposed charge or shape of the holoenzymes; however, these differences are probably subtle because of the extensive conservation of the protein structure among diverse organisms[20,21].

Proteins protect conserved elements in RNAs

To identify the binding site of each protein, phosphorothioate-iodine structure mapping (footprinting) experiments were done with the A- and B-type RNase P RNAs in complex with the *E. coli*, *B. subtilis* or *T. maritima* RNase P protein. To compare A- and B-type holoenzymes in their homogeneous, monomeric states, we trapped specific complexes by nondenaturing gel electrophoresis (**Fig. 1b**). The RNA (modified with phosphorothioates) was then subjected to iodine cleavage within the nondenaturing gel (**Fig. 1b**), and the reaction was quenched before elution of the RNA from each gel band. This technique eliminates the complications of RNA conformational heterogeneity and holoenzyme aggregation and ensures that the footprinting experiments are conducted with RNA that is fully bound by protein.

The *E. coli*, *B. subtilis* and *T. maritima* RNase P proteins protect residues located in helices P2, P3 and at the periphery of P4 in both *B. stearothermophilus* and *E. coli* RNAs (**Fig. 1c,d** and **Supplementary Table 1** online). The data reported were obtained using the catalytic-domain RNAs; no additional residues were protected in the full-length RNAs (data not shown; see Methods). In *B. stearothermophilus* RNA there are a total of 23 residues protected by at least one of the proteins, 17 of which are protected by at least two of the proteins and 14 of which are protected by all three proteins. The amino acid sequences of the RNase P proteins are <30% identical, and variability in the protein protection patterns could reflect subtle differences in the RNA-protein interfaces of each holoenzyme. For example, all three proteins protect residues in helices P2 and P3 of *B. stearothermophilus* RNA, but the *E. coli* protein causes the strongest protection of C23, whereas the *T. maritima* most strongly protects C26 and the *B. subtilis* protein weakly protects both of these residues but uniquely causes increased cleavage of G22 (**Fig. 1c**). Notably, the three proteins show a more consistent footprint in the region of helix P4 (**Fig. 1c** and **Supplementary Table 1**), which is highly conserved among RNase P RNAs. However, the *T. maritima* protein yields the strongest protection pattern (**Fig. 1c,d**), and the *B. subtilis* protein only weakly protects the *E. coli* RNA at the residues listed in **Supplementary Table 1**. The stronger protection by *T. maritima* protein could reflect a more compact holoenzyme structure (consistent with **Figure 1b**) or specific properties of the thermophilic protein, such as conformational rigidity; we do not explore these possibilities in the current analysis.

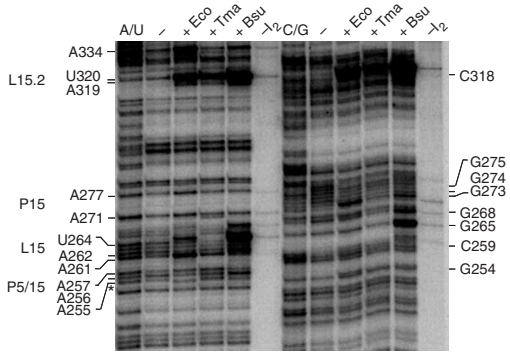

Figure 2 Increased phosphorothioate-iodine cleavage of residues in *B. stearothermophilus* RNA in the presence of proteins. The first lane is denatured RNA (A/U and C/G denote which phosphorothioates are incorporated in the RNA in each panel), the next lanes are RNA in the absence (–) or presence (+) of each of the proteins, and the fifth lane ($-I_2$) is RNA that was not incubated with iodine. The asterisks indicate residues that have two reaction products.

At residues C23, C26 and A49 in the *B. stearothermophilus* RNA, a second reaction product also results from iodine cleavage (**Fig. 1c**). According to the reaction mechanism postulated for phosphorothioate-iodine cleavage[22], the first product presumably contains a 2′,3′-cyclic phosphate. We postulate that the second product contains a 2′ or 3′ phosphate that is derived from a hydrolytic degradation of the first. This is consistent with the difference in the gel mobilities of the two products[23]. The protein apparently affects the formation of the second product (**Fig. 1c**); this suggests that the protein influences specific structural properties of the RNA, which are unclear at this time but may involve coordination of other ligands (for example, Mg^{2+}).

Proteins influence conformation of the RNAs

Examination of the phosphorothioate-iodine data reveals several residues in the RNA that become more prone to cleavage in the presence of protein (**Fig. 2**). These residues are mapped onto the secondary structures of the RNAs in **Figure 3** (cyan); the residues that are protected by protein are shown in red. In the *B. stearothermophilus* RNA, the residues that show increased cleavage in the presence of protein are in the joining region between helix P5 and P15 (J5/15), the loop at the end of helix P15 (L15) and the loop at the end of helix P15.2 (L15.2). Similar protein effects are seen in the homologous regions of *E. coli* RNA (**Fig. 3** and **Supplementary Table 1**) and suggest a conserved link between protein binding and the conformation of the RNA structure in this area. This region of the RNA (adjacent to the protein-binding site) has been implicated in binding tRNA, according to extensive biochemical data[24,25]. In particular, the reactive phosphate of tRNA cross-links to residues in J5/15 in both *E. coli* and *B. subtilis* RNase P RNAs, and there is strong evidence that L15 (J15/16 in *E. coli*) interacts with the 3′ CCA sequence of tRNA. Residues in L15 have also been suggested to coordinate divalent metal ions involved in substrate binding and activity[26,27]. Some of the residues in this region seem to become more prone to Mg^{2+} hydrolysis in the presence of protein (**Supplementary Table 1**), consistent with a previous report about the location of Mg^{2+} hydrolysis sites in *E. coli* RNase P RNA[28]. It is probable, therefore, that the protein influences both the conformation and the metal coordination of L15 (J15/16) in B- and A-type RNAs.

Three of the residues in L15 that are influenced by protein (G265, G268 and A271) are disordered in the crystal structure and may be dynamic in conformation in the absence of substrate, protein or both. There is also variability in the protein effects on residues in J5/15 in *B. stearothermophilus* RNA (for example, A255, A256 and A257; **Fig. 2**); this could reflect a dynamic conformation of the RNA

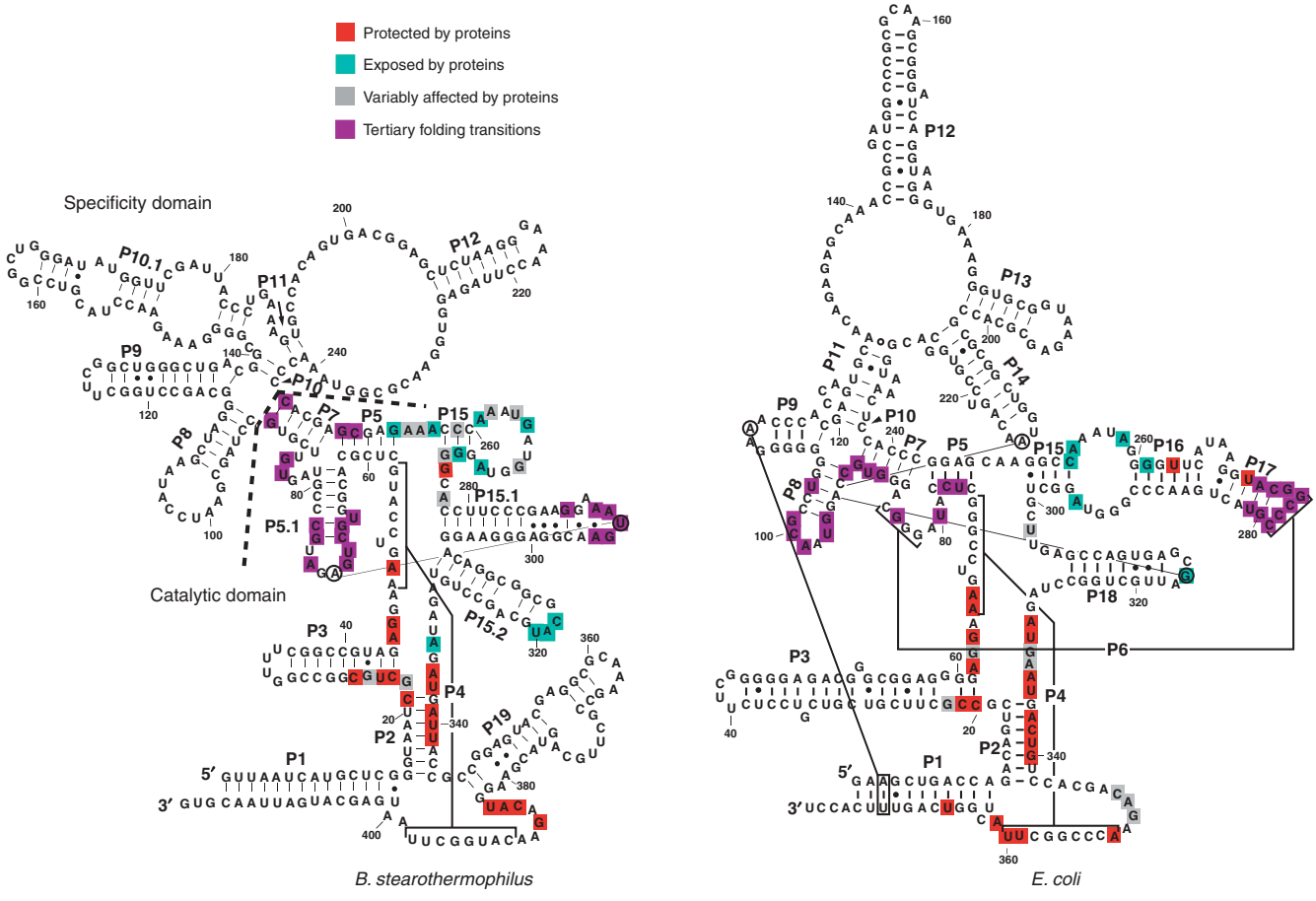

Figure 3 Phosphorothioate-iodine data mapped onto the secondary structures of *B. stearothermophilus* and *E. coli* RNAs. Residues highlighted in red are protected from cleavage by at least two of the three proteins; cyan highlights residues whose cleavage is increased by at least two of the three proteins; gray highlights residues whose cleavage is either protected or increased by only one protein, or where two proteins have opposite effects on the cleavage of the residue (**Supplementary Table 1**). Magenta highlights residues whose cleavage pattern is different in the I and N folding states of the RNA (**Supplementary Table 2**). Tertiary interactions earlier predicted by phylogenetic covariation are indicated with lines between specific residues or structural elements. The catalytic and specificity domains are separated with a dashed line.

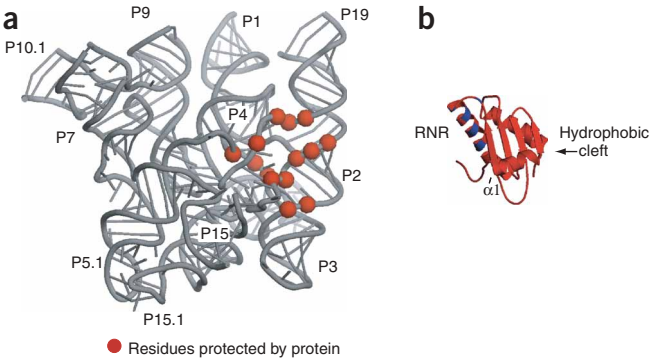

Figure 4 Protection of RNase P RNA by RNase P protein. (**a**) Structure of the *B. stearothermophilus* RNA (298 of 417 nt)[5]. Residues protected by all three proteins are marked with red spheres at the location of the phosphate atoms. (**b**) Structure of the *B. subtilis* protein[21] with the RNR motif and hydrophobic cleft indicated. Residues highlighted in blue (K53, A57, R60, K64, R68) were earlier proposed to be in proximity to RNase P RNA on the basis of site-directed hydroxyl-radical studies[15,16].

structure or could be propagated from slightly different RNA-protein interfaces, as suggested earlier. The influence of the protein on L15.2 is not easily interpreted in our model, because helix P15.2 is pointed away from the core of the RNA and is involved in crystal contacts[5]. However, according to low-resolution cross-linking models of RNase P RNA, the position of L15.2 could be affected by structural changes around P4 (refs. 25,29), which may accompany protein binding (see also **Supplementary Video 1** online).

Ternary complex model

The protection data localize the protein-binding site to residues in conserved, homologous regions of *E. coli* and *B. stearothermophilus* RNAs (**Fig. 3**, red). The protected residues clearly come together in the tertiary structure of the RNA and occupy a patch of structure approximately the same size as the protein (**Fig. 4a**). The structure of the *B. subtilis* protein was previously solved at a resolution of 2.6 Å (ref. 21) and is used here to build the model of the holoenzyme (**Fig. 4b**); the RNase P protein from *B. stearothermophilus* has not yet been identified but is expected to be highly similar in structure[20].

Several features of the RNase P protein are presumed to be important for RNase P RNA or pre-tRNA recognition (**Fig. 4b**). The first is a conserved patch (~11 residues) of highly basic amino acid residues, known as the RNR motif. This structural element occurs in all of the bacterial RNase P proteins identified and is part of an unusual, left-handed βαβ crossover; this topology is also found in the RNA-binding regions of ribosomal protein S5 and ribosomal elongation factor G (ref. 21). Previous site-directed hydroxyl-radical studies with the *E. coli* holoenzyme identified specific residues in the RNR motif that are in proximity (<14 ± 10 Å) to RNase P RNA[15,16]. The positions of the homologous residues are noted on the *B. subtilis* protein structure (**Fig. 4b**, blue) and suggest that this face of the protein is oriented toward the RNA in the holoenzyme. The second conserved feature of the protein is a hydrophobic cleft that is formed by helix α1 and the face of the central β-sheet (20 Å long, 10 Å wide). In a previous report with the *B. subtilis* RNase P protein, residues in this hydrophobic cleft were shown to cross-link to the –4 to –8 positions of the 5′ leader sequence of pre-tRNA[30].

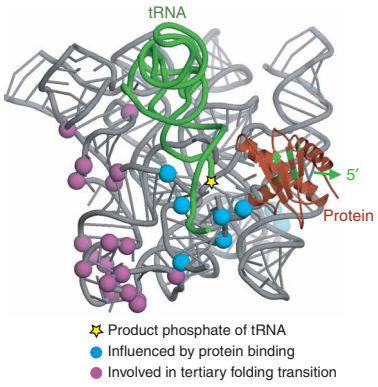

According to the protection data of the current study, the RNase P protein is positioned adjacent to the postulated binding site of tRNA in the ternary complex (**Fig. 5** and **Supplementary Video 1**). We model the tRNA according to a recent report[5], where extensive photoaffinity cross-linking data were used to position the tRNA on the RNA structure. The protein does not reside in the immediate vicinity of the reactive phosphate, consistent with its indirect, rather than direct, role in catalysis. The orientation of the protein places the RNR motif near helices P2 and P4 of RNase P RNA, consistent with constraints indicated by previous hydroxyl-radical mapping data and the low-resolution model of the *E. coli* holoenzyme[15,16]. Given the distance between the hydrophobic cleft of the protein and the cleavage site in pre-tRNA (**Fig. 5**), the protein could interact with 5′ leader sequences longer than 3 or 4 nt, as suggested[16,30,31]. Amino acid residues that were shown to cross-link to the 5′ leader sequence (>4 nt from the cleavage site)[30] are highlighted (**Fig. 5**, green) and provide a potential binding site for the 5′ leader sequence of pre-tRNA.

Linkage between protein binding and RNA folding

Previous studies have shown that the thermodynamic folding pathway of RNase P RNA involves at least three species, unfolded (U), intermediate (I) and native (N): U ↔ I ↔ N. The first transition is characterized by the formation of secondary structure, whereas the second transition involves tertiary structure formation and the cooperative binding of several Mg^{2+} ions; the second transition (I ↔ N) correlates with the formation of the active RNA structure[32,33]. We recently showed that the protein increases the stability of the N state relative to the I state in the *E. coli* holoenzyme, but not in the *B. subtilis* holoenzyme[4]. To examine the structural linkage between the protein-binding site and the tertiary elements involved in the I ↔ N transition, we used the same in-gel phosphorothioate-iodine assay described earlier. The I and N structures of *E. coli* and *B. stearothermophilus* RNAs were separated and probed in a semidenaturing gel (**Fig. 6a**). The energetics of the I ↔ N folding transition are the same in full-length and catalytic-domain *B. stearothermophilus* RNAs

Figure 5 Ternary complex model. The tRNA (green) is modeled on the holoenzyme as described elsewhere[5]. RNA residues that show increased cleavage by at least two of the three proteins are highlighted in cyan (highlighted residues in L15.2 are on the opposite face of the RNA and can be seen in **Supplementary Video 1**); residues whose cleavage pattern differs between the I and N folding states are highlighted in magenta. The *B. subtilis* protein is shown in red; residues highlighted in green (F16, F20, A27, V32, Y34, I86) were earlier shown to cross-link to the 5′ leader sequences of tRNA that were longer than 4 nt[30]. A potential path for the 5′ leader of pre-tRNA is depicted with a green arrow.

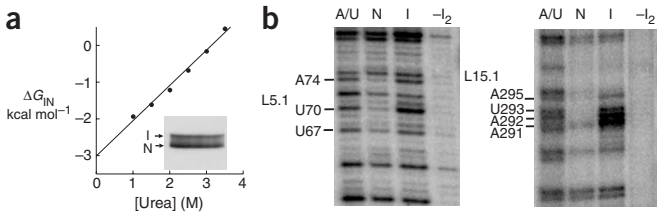

Figure 6 Folding transition of the *B. stearothermophilus* RNA. (**a**) Free-energy difference between the N and I folding states of *B. stearothermophilus* catalytic-domain RNA at 1.0 mM Mg^{2+}. Inset shows partitioning of the I and N states in 3.25 M urea, 1.0 mM Mg^{2+} and 1× THE (pH 7.4) at 10 °C. (**b**) Phosphorothioate-iodine cleavage of the I and N states isolated from the gel shown in **a**.

(ΔG_{IN} = –3.0 ± 0.3 kcal mol^{-1} at 1.0 mM Mg^{2+}, **Fig. 6a**; data collected are for the catalytic-domain RNA). In the *B. stearothermophilus* RNA, a total of 17 residues were more susceptible to iodine cleavage in the I state than in the N state; 3 residues showed the reverse pattern. Similar results were obtained with the *E. coli* RNA, where 19 residues were more exposed and 4 residues less exposed in the I state versus the N state (**Supplementary Table 2** online). An example of the data is shown in **Figure 6**, and the results are highlighted on the secondary structure in **Figure 3** and on the ternary complex in **Figure 5** (magenta).

The main elements involved in the I ↔ N transition of the *B. stearothermophilus* RNA are L5.1 and L15.1. These had earlier been predicted to interact with each other on the basis of phylogenetic analysis[18], as depicted in the secondary structure (**Fig. 3**). Several residues in P5 and P7 are also involved in the B-type transition; this region could either be linked to the L5.1-L15.1 interaction or be independently influenced by urea in the assay. The L5.1 and L15.1 elements are not in proximity to the protein-binding site (**Fig. 5**) and do not occur in the A-type secondary structure (**Fig. 3**). Rather, residues involved in the A-type transition occur in the loop between P5 and P7 and the loop at the end of P17 (which together make up helix P6), in helix P7 and in the loop at the end of helix P8 (**Fig. 3**). Previous low-resolution structural models of the RNAs predicted that the L5.1-L15.1 interaction in the B-type RNA occupies the same spaces as helix P6 in the A-type RNA[25,29,34]. According to our data, the different A- and B-type tertiary elements make similar energetic contributions to the native RNA structures (ΔG_{IN} = −3.0 and −2.3 kcal mol^{-1} at 1.0 mM Mg^{2+} for *B. stearothermophilus* and *E. coli* RNAs, respectively; **Fig. 6a** and data not shown). We earlier showed that the protein influences the stability of these tertiary interactions in the A-type but not the B-type holoenzyme[4]. It is possible, therefore, that the linkage between protein binding and the global folding of the RNA may vary among different bacteria. It is also possible that additional folding transitions are influenced by the proteins, which we do not detect in our assays.

DISCUSSION

We conclude that the bacterial RNase P protein binds to a local, conserved region of RNase P RNA and influences the conformation of adjacent RNA structure that contacts tRNA. Indeed, two regions of the RNA are affected by protein binding. The first is the protein-binding site, defined by a conserved patch of residues protected from iodine cleavage by all of the RNase P proteins examined (**Fig. 4**, red). The second region is adjacent to the binding site and shows altered structural properties in the presence of protein (**Fig. 5**, cyan). In this second region the protein primarily causes increased cleavage of residues, because of increased solvent accessibility, Mg^{2+} hydrolysis of the RNA backbone or both (**Fig. 2** and **Supplementary Table 1**). A previous nucleotide-analog interference mapping study has indicated that mutation of residues in both of these regions of *B. subtilis* RNA influences protein binding[7]. Extensive biochemical data suggest that the region of the RNA adjacent to the protein-binding site contacts tRNA, as represented in the ternary complex model (**Fig. 5**, cyan). This region of the RNA structure may also be linked to catalysis, but the mechanism of catalysis, which is expected to involve Mg^{2+} ions[35,36], cannot be deduced from the structure.

A large conformational change in the RNA does not seem to be required for the protein to bind, because the protein covers roughly the same area as the protection data on the structure (**Fig. 4**). However, some local conformational rearrangement of the RNA is expected to accompany protein binding and propagate into the adjacent region of RNA structure (cyan in **Fig. 5**; discussed earlier). The association rate of the RNase P protein was reported to be 10- to 100-fold slower than expected for diffusion-controlled binding[37]; this implies a rate-limiting step in binding, which would be consistent with a conformational rearrangement of either the RNA or the protein. Such conformational changes are known to occur in other ribonucleoprotein complexes (for example, the signal recognition particle and the ribosome), where induced fit is considered to be important in specific assembly processes[38]. Stabilization of a particular RNA conformation at the protein-binding site could influence both the substrate-binding and catalytic properties of RNase P; this might explain the reduced Mg^{2+} requirement for the maximal cleavage rate by the holoenzyme compared with the RNA alone[39]. According to the models presented here and elsewhere[15,16], the conserved RNR motif of the protein is in close proximity to helix P4, which has been shown in several studies to coordinate Mg^{2+} ions important for catalysis[40–42].

Several studies have been directed at the role of the protein in enhancing the affinity of RNase P for pre-tRNA compared with 5′-matured tRNA. Kinetic and photoaffinity cross-linking experiments suggest that the RNase P protein contacts the 5′ leader sequence of pre-tRNA at positions at least 4 nt from the cleavage site[3,16,30,31]. We earlier showed that the RNA has an important role in substrate recognition by the holoenzyme[4], and there are also biochemical data that suggest interactions between RNase P RNA and the first few nucleotides of the 5′ leader sequence[43–46]. According to the ternary complex model (**Fig. 5**), the protein could affect 5′ leader recognition both directly and indirectly. For example, the protein alters the conformation of the RNA structure near the cleavage site (**Fig. 2**), and this could indirectly affect potential interactions between the RNA and the 5′ leader in this vicinity[44,45,47]. The conserved hydrophobic cleft of the protein might also interact directly with 5′ leader sequences that are longer than 3 or 4 nt. Interactions between the protein and the 5′ leader have been proposed to influence the affinity of Mg^{2+} ions required for catalysis[39]; a link between these two factors might involve a specific orientation of the 5′ leader sequence in the protein cleft. However, further structural and biochemical data are needed to deduce the importance and generality of interactions between the protein and the 5′ leader sequence for all the substrates of RNase P. The primary, conserved function of the protein seems to be stabilization of the RNase P RNA conformation at the tRNA-binding site. Protein recognition of 5′ pre-tRNA leader sequences and protein stabilization of the global RNA structure are probably additional properties of the holoenzyme that could vary among RNase P from different organisms.

METHODS

RNA and protein preparation. *E. coli* and *B. stearothermophilus* catalytic-domain and full-length RNase P RNAs were transcribed *in vitro* from linearized plasmids pEcoΔ and pBstΔ (**Supplementary Methods** online), and pDW98 and BstHH2 (ref. 5). For the footprinting assays, phosphorothioates were randomly incorporated into the RNAs by inclusion of either 0.05 mM CTP [αS] and GTP [αS] or ATP [αS] and UTP [αS] (Sp isomers, Amersham & Invitrogen) in the transcription reactions with 1 mM unmodified nucleotides. RNAs were 5′ end–labeled with T4 polynucleotide kinase (Fisher) and [γ-^{32}P]ATP (MP Biomedicals). Both the RNAs and proteins were purified as described[4].

Nondenaturing gel shift assays. RNase P RNA (5′ end–labeled) was prefolded (0.1 nM ≈ 300 c.p.m. μl^{-1}) in 1× reconstitution buffer: 66 mM HEPES, 33 mM Tris (pH 7.4), 0.1 mM EDTA (1× THE), 100 mM ammonium acetate, 10 mM $MgCl_2$ and 0.05% (v/v) NP-40 for 10 min at 50 °C, followed by 20 min at 37 °C. The RNA was then diluted into an equal volume of RNase P protein (between 0.04 and 20 nM) in the same buffer for an additional 30 min at 37 °C, followed by slow cooling to room temperature. Before loading, 50% (v/v) glycerol was added to a final concentration of 5%, and the samples were either loaded directly onto a nondenaturing gel (1× THE (pH 7.4), 1.0 mM $MgCl_2$ and 4.5% (w/v) acrylamide) or incubated overnight at 4 °C and then loaded onto the gel (this comparison confirmed that the reactions had come to equilibrium). The gels ran for 3.5 h at 350 V (with an internal temperature of 10 °C), after which they were dried and visualized with a Phosphorimager (Molecular Dynamics). The fraction of RNA bound to protein [R-P] was quantified at each protein concentration and plotted according to $[R\text{-}P]/[R]_{total} = 1/(1 + K_d/[P]_{total})$. The nondenaturing gel shift experiments were also conducted with 50 nM RNA and 0, 0.5, 1, 1.5 and 2× protein to ensure that the *B. subtilis*, *E. coli* and *T. maritima* RNase P proteins bound with the same stoichiometry to the RNAs. With certain protein stocks, ~1.5× protein was required to bind all the RNA, presumably because of a portion of inactive protein.

In-gel phosphorothioate-iodine footprinting. The data shown (**Figs. 1** and **2** and **Supplementary Table 1**) were obtained with catalytic-domain RNase P RNAs; the first ~10 nt of the 5′ and 3′ ends were not examined. Results with full-length RNase P RNAs were the same as for the catalytic-domain RNAs, with a few exceptions that are noted in **Supplementary Methods**. In all experiments, the RNAs (~50 nM) with randomly incorporated phosphorothioates were incubated in 1× reconstitution buffer and then reconstituted with equimolar (~1–1.5×) RNase P protein as described earlier. The RNAs and holoenzymes were then loaded onto nondenaturing gels (1× THE (pH 7.4), 1.0 mM $MgCl_2$ and 4.5% (w/v) acrylamide at 10 °C) that were run as described earlier. The samples rapidly equilibrated to the conditions of the gel (data not shown), and the protein footprint was, therefore, mapped at 1.0 mM Mg^{2+}. A detailed description of the in-gel and solution footprinting methods is given in **Supplementary Methods**. To characterize the folding states of the RNAs, urea gradient–denaturing gel electrophoresis was carried out and the ΔG_{IN} values were calculated at each urea concentration according to $\Delta G_{IN} = -RT \ln([N]/[I])$, as described previously[4]. The ΔG_{IN} at zero urea was obtained by linear extrapolation. The I and N states of the *B. stearothermophilus* and *E. coli* RNase P RNAs were separated in gels that contained 1× THE (pH 7.4), 1.0 mM $MgCl_2$, 4.5% (w/v) acrylamide and either 3.25 or 1.75 M urea, respectively; the I and N states of the RNAs were then subjected to the in-gel structure-mapping assay.

Structural models and graphics. The protein structure was modeled onto the RNase P RNA structure using O[48] and Insight2 (Molecular Simulations, Inc.). Graphics were generated with Insight2 and PyMOL (http://pymol.sourceforge.net). The coordinates of the ternary complex model are available on the RNase P database (http://jwbrown.mbio.ncsu.edu/RNaseP/home.html)[49].

Note: Supplementary information is available on the Nature Structural & Molecular Biology website.

ACKNOWLEDGMENTS

We thank A. Krivenko for cloning and initial characterization of the catalytic-domain constructs. We thank R. Batey for helpful comments regarding this work. The research was supported by The US National Institutes of Health (grant GM-34527 to N.R.P. and Molecular Biophysics Training Grant T32 GM-65103 to A.H.B.) through the University of Colorado at Boulder.

COMPETING INTERESTS STATEMENT

The authors declare that they have no competing financial interests.

Published online at http://www.nature.com/nsmb/
Reprints and permissions information is available online at http://npg.nature.com/reprintsandpermissions/

1. Guerrier-Takada, C., Gardiner, K., Marsh, T., Pace, N. & Altman, S. The RNA moiety of ribonuclease P is the catalytic subunit of the enzyme. *Cell* **35**, 849–857 (1983).
2. Reich, C., Olsen, G.J., Pace, B. & Pace, N.R. Role of the protein moiety of ribonuclease P, a ribonucleoprotein enzyme. *Science* **239**, 178–181 (1988).
3. Kurz, J.C., Niranjanakumari, S. & Fierke, C.A. Protein component of *Bacillus subtilis* RNase P specifically enhances the affinity for precursor-tRNA^{Asp}. *Biochemistry* **37**, 2393–2400 (1998).
4. Buck, A.H., Dalby, A.B., Poole, A., Kazantsev, A.V. & Pace, N.R. Protein activation of a ribozyme: the role of bacterial RNase P protein. *EMBO J.* published online 15 September 2005 (doi:10.1038/sj.emboj.7600805).
5. Kazantsev, A.V. *et al.* Crystal structure of a bacterial ribonuclease P RNA. *Proc. Natl. Acad. Sci. USA* **102**, 13392–13397 (2005).
6. Loria, A., Niranjanakumari, S., Fierke, C.A. & Pan, T. Recognition of a pre-tRNA substrate by the *Bacillus subtilis* RNase P holoenzyme. *Biochemistry* **37**, 15466–15473 (1998).
7. Rox, C., Feltens, R., Pfeiffer, T. & Hartmann, R.K. Potential contact sites between the protein and RNA subunit in the *Bacillus subtilis* RNase P holoenzyme. *J. Mol. Biol.* **315**, 551–560 (2002).
8. Day-Storms, J.J., Niranjanakumari, S. & Fierke, C.A. Ionic interactions between PRNA and P protein in *Bacillus subtilis* RNase P characterized using a magnetocapture-based assay. *RNA* **10**, 1595–1608 (2004).
9. Loria, A. & Pan, T. Modular construction for function of a ribonucleoprotein enzyme: the catalytic domain of *Bacillus subtilis* RNase P complexed with *B. subtilis* RNase P protein. *Nucleic Acids Res.* **29**, 1892–1897 (2001).
10. Waugh, D.S. & Pace, N.R. Complementation of an RNase P RNA (rnpB) gene deletion in *Escherichia coli* by homologous genes from distantly related eubacteria. *J. Bacteriol.* **172**, 6316–6322 (1990).
11. Vioque, A., Arnez, J. & Altman, S. Protein-RNA interactions in the RNase P holoenzyme from *Escherichia coli*. *J. Mol. Biol.* **202**, 835–848 (1988).
12. Talbot, S.J. & Altman, S. Gel retardation analysis of the interaction between C5 protein and M1 RNA in the formation of the ribonuclease P holoenzyme from *Escherichia coli*. *Biochemistry* **33**, 1399–1405 (1994).
13. Westhof, E., Wesolowski, D. & Altman, S. Mapping in three dimensions of regions in a catalytic RNA protected from attack by an Fe(II)-EDTA reagent. *J. Mol. Biol.* **258**, 600–613 (1996).
14. Sharkady, S.M. & Nolan, J.M. Bacterial ribonuclease P holoenzyme crosslinking analysis reveals protein interaction sites on the RNA subunit. *Nucleic Acids Res.* **29**, 3848–3856 (2001).
15. Biswas, R., Ledman, D.W., Fox, R.O., Altman, S. & Gopalan, V. Mapping RNA-protein interactions in ribonuclease P from *Escherichia coli* using disulfide-linked EDTA-Fe. *J. Mol. Biol.* **296**, 19–31 (2000).
16. Tsai, H.Y., Masquida, B., Biswas, R., Westhof, E. & Gopalan, V. Molecular modeling of the three-dimensional structure of the bacterial RNase P holoenzyme. *J. Mol. Biol.* **325**, 661–675 (2003).
17. Fang, X.W. *et al.* The *Bacillus subtilis* RNase P holoenzyme contains two RNase P RNA and two RNase P protein subunits. *RNA* **7**, 233–241 (2001).
18. Haas, E.S., Banta, A.B., Harris, J.K., Pace, N.R. & Brown, J.W. Structure and evolution of ribonuclease P RNA in Gram-positive bacteria. *Nucleic Acids Res.* **24**, 4775–4782 (1996).
19. Brown, J.W. & Pace, N.R. Ribonuclease P RNA and protein subunits from bacteria. *Nucleic Acids Res.* **20**, 1451–1456 (1992).
20. Kazantsev, A.V. *et al.* High-resolution structure of RNase P protein from *Thermotoga maritima*. *Proc. Natl. Acad. Sci. USA* **100**, 7497–7502 (2003).
21. Stams, T., Niranjanakumari, S., Fierke, C.A. & Christianson, D.W. Ribonuclease P protein structure: evolutionary origins in the translational apparatus. *Science* **280**, 752–755 (1998).
22. Gish, G. & Eckstein, F. DNA and RNA sequence determination based on phosphorothioate chemistry. *Science* **240**, 1520–1522 (1988).
23. Winkler, W.C., Nahvi, A., Roth, A., Collins, J.A. & Breaker, R.R. Control of gene expression by a natural metabolite-responsive ribozyme. *Nature* **428**, 281–286 (2004).
24. Christian, E.L., Zahler, N.H., Kaye, N.M. & Harris, M.E. Analysis of substrate recognition by the ribonucleoprotein endonuclease RNase P. *Methods* **28**, 307–322 (2002).
25. Chen, J.L., Nolan, J.M., Harris, M.E. & Pace, N.R. Comparative photocross-linking analysis of the tertiary structures of *Escherichia coli* and *Bacillus subtilis* RNase P RNAs. *EMBO J.* **17**, 1515–1525 (1998).
26. Kufel, J. & Kirsebom, L.A. The P15-loop of *Escherichia coli* RNase P RNA is an autonomous divalent metal ion binding domain. *RNA* **4**, 777–788 (1998).
27. Oh, B.K., Frank, D.N. & Pace, N.R. Participation of the 3′-CCA of tRNA in the binding of catalytic Mg^{2+} ions by ribonuclease P. *Biochemistry* **37**, 7277–7283 (1998).
28. Kazakov, S. & Altman, S. Site-specific cleavage by metal ion cofactors and inhibitors of M1 RNA, the catalytic subunit of RNase P from *Escherichia coli*. *Proc. Natl. Acad. Sci. USA* **88**, 9193–9197 (1991).

29. Massire, C., Jaeger, L. & Westhof, E. Derivation of the three-dimensional architecture of bacterial ribonuclease P RNAs from comparative sequence analysis. *J. Mol. Biol.* **279**, 773–793 (1998).
30. Niranjanakumari, S., Stams, T., Crary, S.M., Christianson, D.W. & Fierke, C.A. Protein component of the ribozyme ribonuclease P alters substrate recognition by directly contacting precursor tRNA. *Proc. Natl. Acad. Sci. USA* **95**, 15212–15217 (1998).
31. Crary, S.M., Niranjanakumari, S. & Fierke, C.A. The protein component of *Bacillus subtilis* ribonuclease P increases catalytic efficiency by enhancing interactions with the 5′ leader sequence of pre-tRNA^{Asp}. *Biochemistry* **37**, 9409–9416 (1998).
32. Pan, T. & Sosnick, T.R. Intermediates and kinetic traps in the folding of a large ribozyme revealed by circular dichroism and UV absorbance spectroscopies and catalytic activity. *Nat. Struct. Biol.* **4**, 931–938 (1997).
33. Fang, X., Pan, T. & Sosnick, T.R. A thermodynamic framework and cooperativity in the tertiary folding of a Mg^{2+}-dependent ribozyme. *Biochemistry* **38**, 16840–16846 (1999).
34. Haas, E.S., Morse, D.P., Brown, J.W., Schmidt, F.J. & Pace, N.R. Long-range structure in ribonuclease P RNA. *Science* **254**, 853–856 (1991).
35. Beebe, J.A. & Fierke, C.A. A kinetic mechanism for cleavage of precursor tRNA^{Asp} catalyzed by the RNA component of *Bacillus subtilis* ribonuclease P. *Biochemistry* **33**, 10294–10304 (1994).
36. Smith, D. & Pace, N.R. Multiple magnesium ions in the ribonuclease P reaction mechanism. *Biochemistry* **32**, 5273–5281 (1993).
37. Talbot, S.J. & Altman, S. Kinetic and thermodynamic analysis of RNA-protein interactions in the RNase P holoenzyme from *Escherichia coli*. *Biochemistry* **33**, 1406–1411 (1994).
38. Williamson, J.R. Induced fit in RNA-protein recognition. *Nat. Struct. Biol.* **7**, 834–837 (2000).
39. Kurz, J.C. & Fierke, C.A. The affinity of magnesium binding sites in the *Bacillus subtilis* RNase P × pre-tRNA complex is enhanced by the protein subunit. *Biochemistry* **41**, 9545–9558 (2002).
40. Frank, D.N. & Pace, N.R. *In vitro* selection for altered divalent metal specificity in the RNase P RNA. *Proc. Natl. Acad. Sci. USA* **94**, 14355–14360 (1997).
41. Christian, E.L., Kaye, N.M. & Harris, M.E. Helix P4 is a divalent metal ion binding site in the conserved core of the ribonuclease P ribozyme. *RNA* **6**, 511–519 (2000).
42. Crary, S.M., Kurz, J.C. & Fierke, C.A. Specific phosphorothioate substitutions probe the active site of *Bacillus subtilis* ribonuclease P. *RNA* **8**, 933–947 (2002).
43. Brannvall, M., Fredrik Pettersson, B.M. & Kirsebom, L.A. The residue immediately upstream of the RNase P cleavage site is a positive determinant. *Biochimie* **84**, 693–703 (2002).
44. LaGrandeur, T.E., Huttenhofer, A., Noller, H.F. & Pace, N.R. Phylogenetic comparative chemical footprint analysis of the interaction between ribonuclease P RNA and tRNA. *EMBO J.* **13**, 3945–3952 (1994).
45. Zahler, N.H., Christian, E.L. & Harris, M.E. Recognition of the 5′ leader of pre-tRNA substrates by the active site of ribonuclease P. *RNA* **9**, 734–745 (2003).
46. Zuleeg, T. *et al.* Correlation between processing efficiency for ribonuclease P minimal substrates and conformation of the nucleotide –1 at the cleavage position. *Biochemistry* **40**, 3363–3369 (2001).
47. Christian, E.L. & Harris, M.E. The track of the pre-tRNA 5′ leader in the ribonuclease P ribozyme-substrate complex. *Biochemistry* **38**, 12629–12638 (1999).
48. Jones, T.A., Zou, J.Y., Cowan, S.W. & Kjeldgaard, M. Improved methods for building protein models in electron density maps and the location of errors in these models. *Acta Crystallogr. A* **47**, 110–119 (1991).
49. Brown, J.W. The ribonuclease P database. *Nucleic Acids Res.* **27**, 314 (1999).